Chapter 8

DENTAL DEVELOPMENT IN AND AGE AT DEATH OF THE SCLADINA I-4A JUVENILE NEANDERTAL

Tanya M. SMITH, Donald J. REID, Anthony J. OLEJNICZAK, Paul T. TAFFOREAU, Jean-Jacques HUBLIN & Michel TOUSSAINT

Michel Toussaint & Dominique Bonjean (eds.), 2014. The Scladina I-4A Juvenile Neandertal (Andenne, Belgium), Palaeoanthropology and Context
Études et Recherches Archéologiques de l'Université de Liège, 134: 155-166.

1. Introduction

1.1. Dental microstructure and age at death estimation

Dental development in humans and apes begins prior to birth and continues throughout adolescence. Like many biological systems, tooth formation is characterized by a circadian (daily) rhythm (reviewed in Smith, 2006). Teeth grow in a layered fashion through the addition of incremental features (that may be understood by analogy with tree rings), as well as by the progressive activation of secretory cells (reviewed in Boyde, 1989). Developmental rate and time are permanently recorded by these incremental lines in the enamel and dentine, which remain unchanged for millions of years.

Enamel is secreted by cells known as ameloblasts, which differentiate at the enamel-dentine junction and migrate outward towards what becomes the surface of the crown. The tracks left by these individual cells are known as enamel prisms. The prisms show cross-striations that result from the circadian rhythm of enamel secretion (Bromage, 1991; Smith, 2006). The successive positions of the advancing front of forming enamel are preserved as long-period incremental structures termed Retzius lines (Figure 1), which contact the enamel surface and form perikymata (Figure 2). Cross-striations and Retzius lines are also frequently referred to as short- and long-period structures due to their respective 24-hour and greater than 24-hour rhythms (6–12 days in hominins). An important relationship exists between these lines, as the long-period line periodicity (repeat interval or number of days between long-period lines), may only be determined by counting cross-striations between Retzius lines internally. This value is the same for all teeth in an individual's dentition, although it may vary among individuals (FitzGerald, 1998).

Dentine is produced by cells known as odontoblasts that rhythmically produce daily incremental lines known as von Ebner's lines (equivalent to cross-striations), long-period structures known as Andresen lines (equivalent to Retzius lines), and periradicular bands (equivalent to perikymata; Figures 1 & 2; reviewed in Dean, 1995 and Smith, 2008). Counts and measurements of these

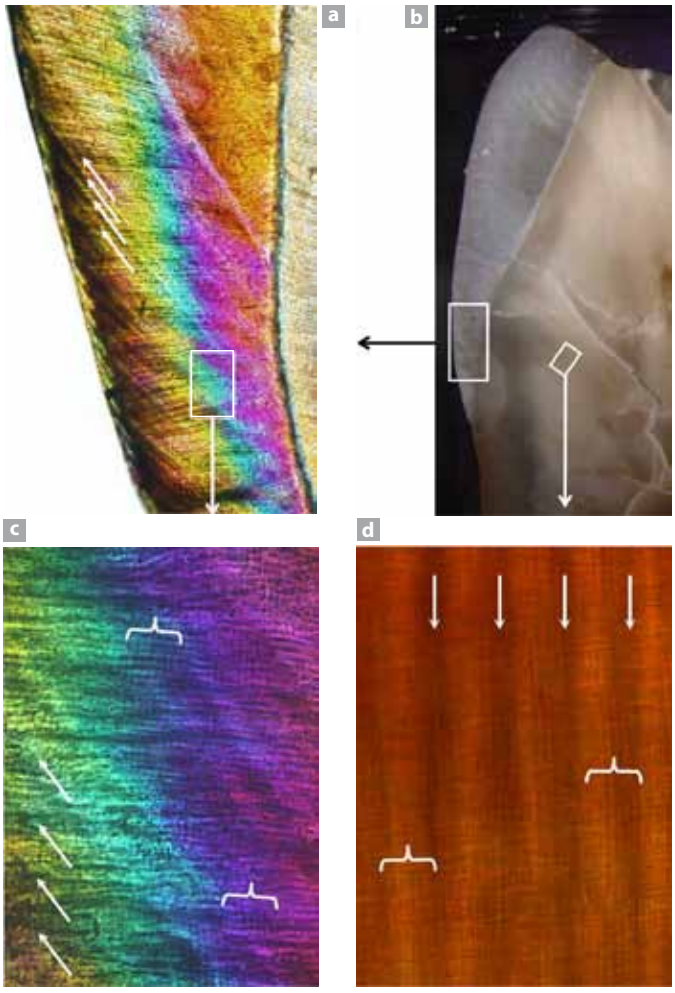

Figure 1: Incremental features found in enamel and dentine. a) Long-period Retzius lines in enamel (arrowed); b) overview of Scladina permanent maxillary right first molar (Scla 4A-4) showing the position of higher magnification images in a) and d); c) Retzius lines (arrowed) and short-period cross-striations in enamel (light and dark bands indicated by brackets); d) Long-period Andresen lines (arrowed) and short-period von Ebner's lines in dentine (light and dark bands indicated by brackets).

Figure 2: Long-period incremental growth lines (indicated by fine dotted lines) on the surface of the mandibular first premolar (Scla 4A-6). a) tooth crown: perikymata, and b) tooth root: periradicular bands.

short- and long-period lines provide information on the rate and duration of enamel and dentine secretion, which may be combined to accurately determine the total crown formation time, and the rate and duration of crown and root extension (e.g., Smith et al., 2006[a]). Furthermore, the age at death in developing dentitions may be precisely determined by identifying the birth line (neonatal line), and adding subsequent crown and root formation time to yield the age.

1.2. Tooth growth and age at death in fossil hominins

In the past few decades, several studies have used information from incremental features preserved in dental tissues to determine age at death, as well as to infer patterns of life history (development scheduling and the timing of reproductive events) in juvenile fossil hominins (e.g., Bromage & Dean, 1985; Dean et al., 1993, 2001; Smith et al., 2007[a,b], 2010). Dental microstructure research on juvenile Neandertals has focused on individuals from Devil's Tower, Gibraltar (Dean et al., 1986; Stringer et al., 1990; Stringer & Dean, 1997; Smith et al., 2010); Hortus, France (Ramirez Rozzi, 2005); Le Moustier, France (Smith et al., 2010); Obi-Rakhmat Grotto, Uzbekistan (Smith et al., 2010, 2011); Engis, Belgium (Smith et al., 2010); Krapina, Croatia (Smith et al., 2010) and an infant from Dederiyeh, Syria (Sasaki et al., 2003). These studies were concerned primarily with determining the age at death from counts of incremental features in the dental enamel.

Other studies have been conducted on the number and spacing of long-period growth lines (perikymata/Retzius lines) in diverse samples of Neandertals and Middle Stone Age and Upper Palaeolithic Modern Humans (Mann et al., 1991; Ramirez Rozzi, 1993; Mann & Vandermeersch, 1997, Ramirez Rozzi & Bermudez de Castro, 2004; Guatelli-Steinberg et al., 2005, 2007[a, b]; Smith et al., 2006[b]; Guatelli-Steinberg & Reid, 2008; Reid et al., 2008), in addition to the study of Neandertal internal enamel development in single permanent molars from Tabun, Israel (Dean et al., 2001; Dean, 2007[a]); La Chaise, France (Macchiarelli et al., 2006); and Lakonis, Greece (Smith et al., 2009). Research on relative dental development in Neandertals has been conducted by Wolpoff (1979), Tompkins (1996), Thompson & Nelson (2000), and Granat & Heim (2003). Most of these studies have suggested that Neandertals show more rapid dental development than modern humans, although Neandertals appear to overlap with the lower end, or shorter-forming portion, of the human range. This distinction is of particular importance for studies that use modern human developmental profiles to assign ages to juvenile Neandertals (e.g., Mann & Vandermeersch, 1997; Tillier, 2000; Coqueugniot & Hublin, 2007; but see Shackelford et al., 2012).

This study aims to assess crown and root formation time of the juvenile Neandertal Scladina I-4A, as well as the age at death. Surface manifestations of long-period incremental features on tooth crowns and roots were quantified, the degree of root formation was assessed, and a first molar tooth was sectioned to determine the long-period line periodicity and to register chronological and developmental time. In addition, a sequence of developmental stress across the dentition was mapped, which allowed registry of teeth forming at the same time, and the estimation of the age at death. These data were compared with data on incremental development in modern humans from northern England and southern Africa, as well as a large sample of Neandertals (Reid & Dean, 2006; Smith et al., 2007[b]; Guatelli-Steinberg & Reid, 2008; Reid et al., 2008).

2. Material and methods

2.1. Preparation

The dental material from the Scladina Juvenile recovered over the past two decades provides an exceptional opportunity to examine isolated but associated teeth, which are described in detail in this volume. For this study, all permanent right tooth types of the Scladina Juvenile were examined, save for the mandibular first premolar, which has yet to be recovered. The first stage in the analysis involved photographic documentation with stereomicroscopy, followed by micro-computed tomographic (micro-CT) scanning with the Skyscan 1076 at Antwerp University (Belgium) and Skyscan 1172 (for selected additional scans) at the Max Planck Institute for Evolutionary Anthropology (Germany). Micro-CT scanning ensured that the entire sample would be accurately preserved digitally, and that the teeth would be available for non-destructive study of enamel thickness (Olejniczak et al., 2008; Smith et al., 2012). High resolution peels and molds of all available permanent teeth were made with Struers' Repliset and Coltene President impression materials, and casts were subsequently prepared with Epo-Tek 301 epoxy resin. The casts were lightly gold coated with a sputter coater for enhanced stereomicroscopic visualization.

In order to determine the long-period line periodicity, a histological thin section of the permanent maxillary right first molar (Scla 4A-4) was prepared. To approximate a plane of section passing through the tips of the mesial dentine horns, a virtual 3D model was generated with Vox Blast Software (Vaytek, Inc.; Figure 3), the dentine horn tips were located, and a virtual plane of section was cut through the mesial cusp tips and dentine horns. The virtual model was used to orient the tooth prior to sectioning, which facilitated the production of a physical section plane that was similar to the 'ideal' virtual plane (Figure 4). In order to stabilize the tooth during sectioning, it was first embedded in methylmethacrylate resin, and then cut with a Logitech annular saw (Figure 5). The thin section was mounted to a microscope slide according to procedures described in Reid et al. (1998). This involved a temporary bond with dental sticky wax, lapping one face with 1 micron alumina, bonding the lapped face with UV-curing resin under pressure, lapping the other face down to approximately 120 microns, and covering the section with a coverslip and DPX mounting media. The remaining tooth was then removed from the methylacrylate resin with dichloromethane and restored to its original appearance with temporary dental restoratives and dental sticky wax (Figure 6). After the two cuts to remove the section for histological preparation, it was estimated that less than 1.5 mm of the specimen's mesial-distal thickness was lost.

Figure 3: Virtual model of permanent maxillary right first molar crown (Scla 4A-4) with the orientation used to produce the least oblique virtual section and to orient the tooth prior to physical sectioning.

Two teeth (Scla 4A-6, Scla 4A-11) were brought to the European Synchrotron Radiation Facility in Grenoble, France in order to confirm results on

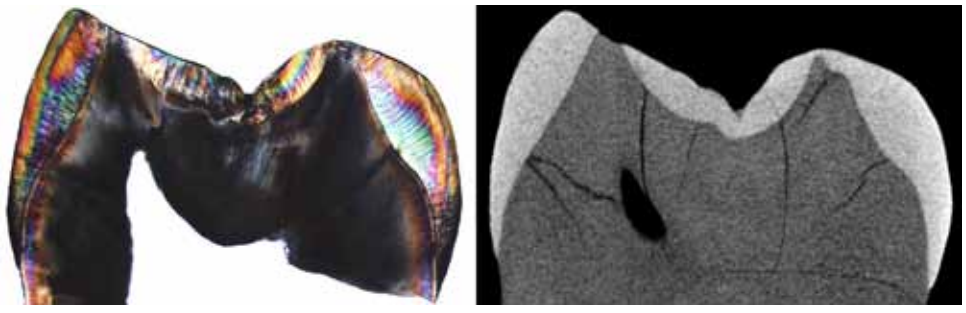

Figure 4: Histological section of the permanent maxillary right first molar crown (Scla 4A-4) (left) compared to the virtual (target) plane of section (right).

the long-period lines periodicity obtained from the physical section of the molar. In order to assess internal features non-destructively, small portions of the mid-lateral enamel of the maxillary right central incisor were scanned using an isotropic 0.7 µm voxel size with propagation phase contrast X-ray synchrotron micro-CT performed on the beamline ID 19 (Figure 7). This technique facilitates non-destructive resolution of dental microstructure (invisible with conventional micro-CT) at the sub-micron level (Tafforeau, 2004; Tafforeau et al., 2006), including the long-period line periodicity (Smith et al., 2007[a], 2010; Smith & Tafforeau, 2008; Tafforeau & Smith, 2008).

These scans were performed with a monochromatic beam at an energy of 52 keV using a multilayer monochromator. The propagation phase effect used to reveal dental microstructure was created with a sample-to-detector distance of

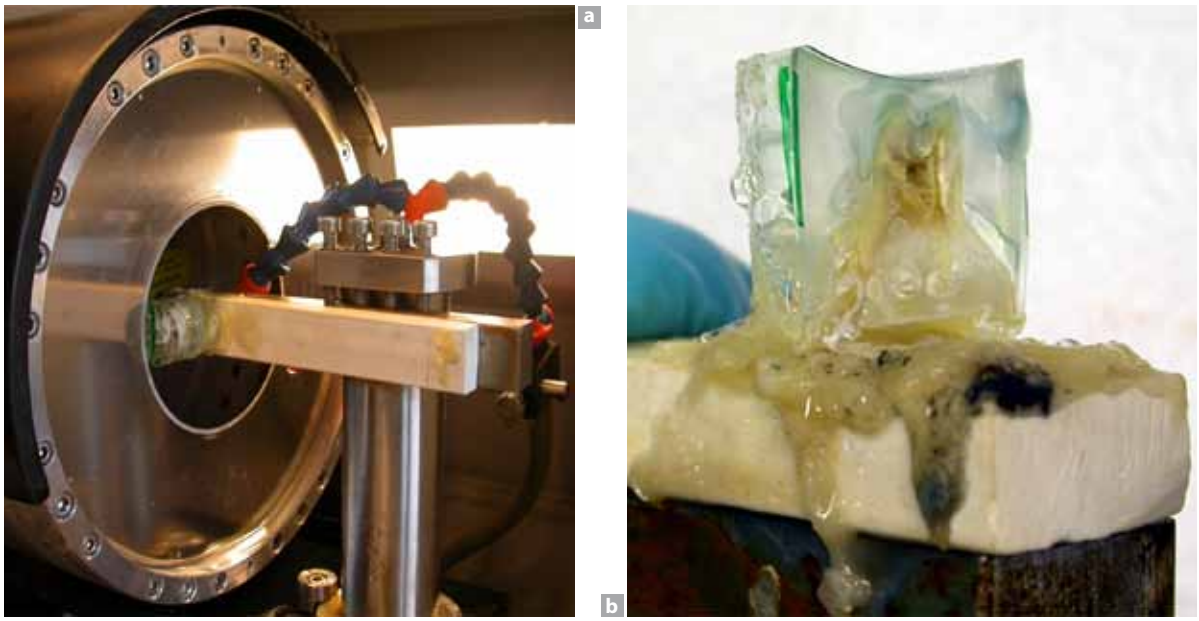

Figure 5: a) The embedded permanent maxillary right first molar (Scla 4A-4) on the annular saw, and b) after the section has been cut.

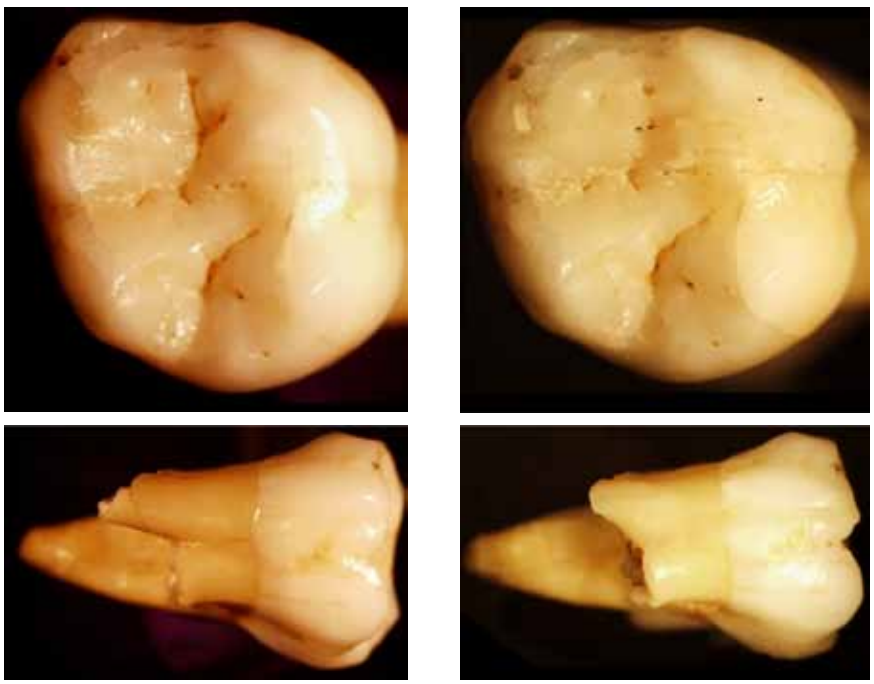

Figure 6: Comparison of the Scladina molar (Scla 4A-4) before (left) and after (right) reconstruction. The small amount of missing root on the right was removed for ancient DNA analysis prior to reconstruction. (Note the orientation and scale is slightly different in the panels.)

150 mm. Strong ring artefacts due to the multi-layer and detector were corrected using four processing steps: conditional flatfield correction, residual horizontal line removal, subtraction of a filtered average of all scan projections (general ring correction), and finally a correction of residual rings on reconstructed slices (adapted from Tafforeau, 2004). Virtual histological slices were prepared using average projections on a virtual thickness of 100 slices (70 µm) after precise alignment along incremental features, following the protocol described in Tafforeau et al. (2007) and Tafforeau & Smith (2008).

2.2. Developmental analysis

Crown formation time was determined from the mesiopalatal cusp (protocone) of the permanent maxillary right first molar according to the procedure described in Boyde (1963, 1990). The neonatal line was identified, and daily cross-striations were counted and/or measured along a prism track from the neonatal line to an accentuated line to yield formation time in days (Figure 8). The accentuated line was tracked down toward the enamel-dentine junction, and the count was continued along a prism to the next accentuated line. This process was repeated until the enamel cervix was reached. It was not possible to determine formation times for cuspal and imbricational regions of the crown (e.g., Reid et al., 1998; Smith, 2008) due to the degree of attrition, which prohibited identification of the beginning of imbricational enamel formation. A particularly marked accentuated line was estimated to have been formed at approximately 435 days of age and matched in the mesiobuccal cusp; 47 Retzius lines were counted after this line to yield the age at mesiobuccal cusp completion. It was not possible to identify a neonatal line in this cusp due to heavy attrition that had worn the enamel away (Figure 4).

Crown formation times for unworn/lightly worn teeth were determined by summing an estimate of cuspal formation time with the total number of perikymata times the periodicity. Cuspal formation time was calculated by two different methods and an average value was determined; a minimum estimate was calculated as cuspal thickness divided by the modern human mean cuspal daily secretion rate: 3.80 µm/day for anterior teeth (Schwartz et al., 2001) and 4.11 µm/day for postcanine teeth (Smith et al., 2007[b]). Linear cuspal enamel thickness was determined from micro-CT slices; measurements were made

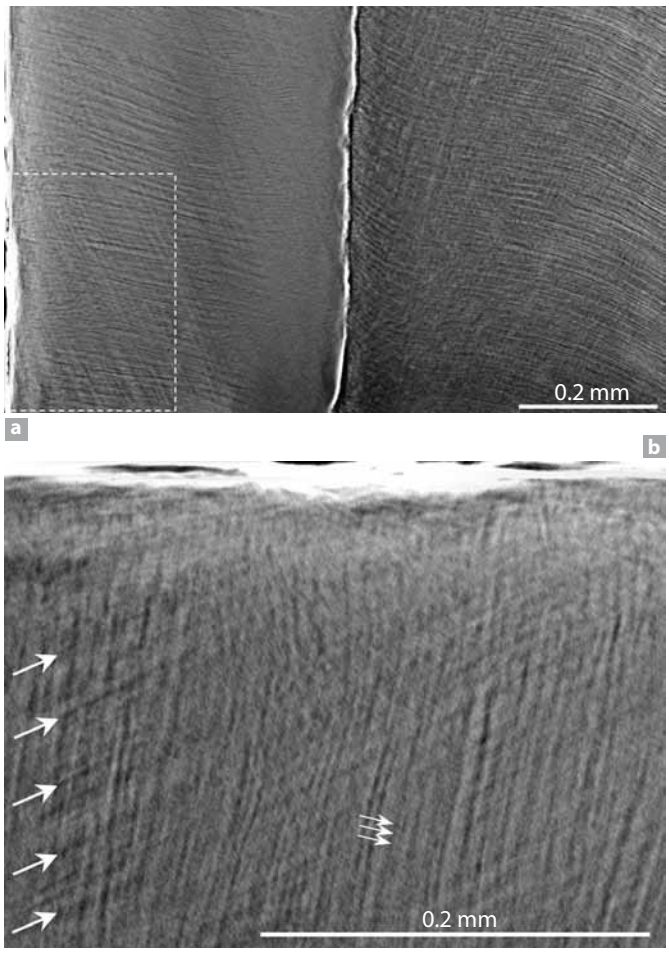

Figure 7: Scladina permanent maxillary right central incisor (Scla 4A-11) scanned with phase-contrast X-ray synchrotron microtomography. a) Overview of enamel (left) and dentine (right), showing an area (dotted box) enlarged in b). b) Developmental features revealed with non-destructive synchrotron imaging: Retzius lines (large arrows) and daily cross-striations (small arrows).

from the tip of the dentine horn to the approximate position of the first perikymata at the cusp surface. A maximum cuspal formation time estimate was calculated with regression equations for anterior and posterior modern human teeth (Dean et al., 2001; Schwartz & Dean, 2001).

Developmental stress in the enamel and dentine of the first molar was mapped, registered to hypoplasias on anterior teeth, and subsequent long-period lines were counted on tooth crowns and roots. Crown initiation ages were determined by subtracting coronal developmental time prior to the known age stress events. Crown completion ages were determined by adding coronal developmental time after the known age stress events. This individual's age at death was determined by adding the time of formation of the first premolar

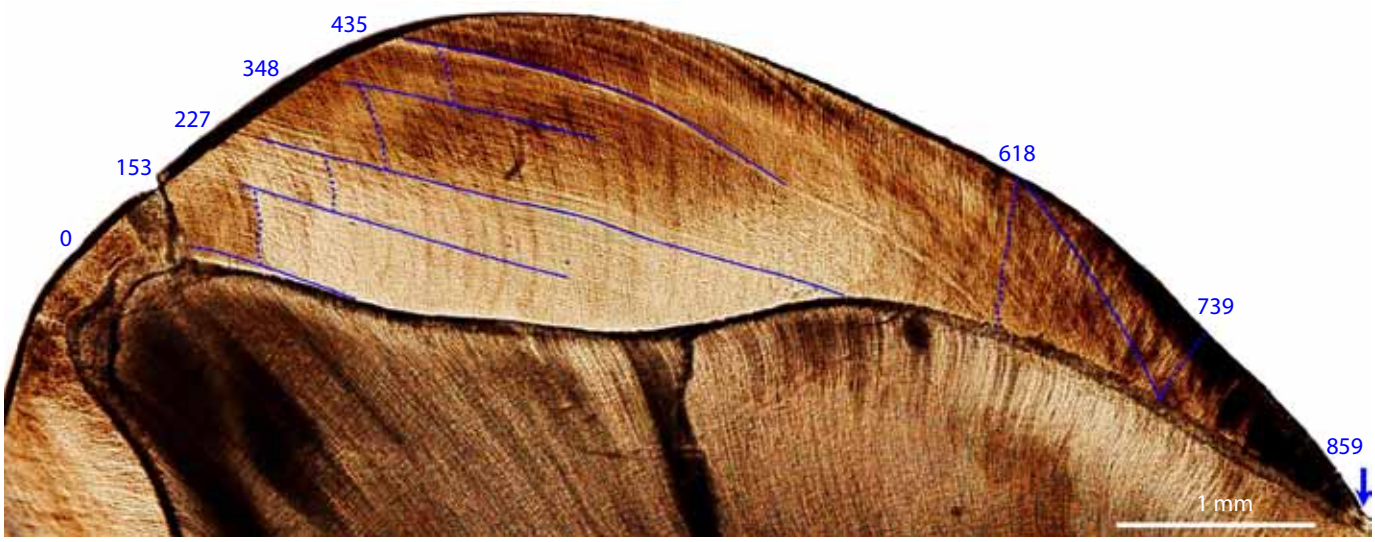

Figure 8: Permanent maxillary right first molar (Scla 4A-4) reconstruction of protocone crown formation time. The neonatal line is indicated by the first blue line on the lower left (0), with subsequent calculated time indicated for a series of stress events as 153 days, 227 days, 348 days, and 435 days postnatal age. The stress event at 435 days (1.19 years) was the most marked until the later stressors at 875 and 1779 days of age (not shown here). The crown was completed at 859 days of age (2.35 years).

after the final registered stress event. The permanent maxillary right third molar initiation age was determined by subtracting the estimated time of crown formation time from the age at death.

For root development, root length was first assessed from casts and photographs of the original teeth, and corrections were made for minor amounts of missing root. Long-period lines (periradicular bands: Smith et al., 2007[b]) were counted from the enamel cervix to the developing edge where possible on peels, casts, and original specimens using 50× or greater magnification. The number of lines was multiplied by the periodicity to determine the formation time in days. The overall rate of root extension was determined by division of the root length (in microns) by the time of formation (in days).

3. Results

The developmental variables for each tooth in the Scladina Juvenile's dentition are given in Table 1. The long-period line periodicity was 8 days in this individual, which was determined in both the histological section of the permanent maxillary right first molar and the virtual section of the permanent maxillary right central incisor imaged with phase contrast synchrotron microtomography. The permanent maxillary right first molar showed a neonatal (birth) line 13 days after mesiopalatal cusp initiation (Figure 7), which allowed subsequent developmental time to be registered to chronological age. Crown formation time of the mesiopalatal cusp was approximately 872 days, and ages at cuspal crown completion were 2.35 years and 2.22 years for the mesiopalatal and mesiobuccal cusps, respectively. A chronology of developmental stress was identified in the enamel and dentine of the first molar at approximately 435, 875, and 1779 days of age, which was matched across anterior teeth (Figure 9). The final known-age developmental stress (at 1779 days of age) in the developing mandibular first premolar was used to establish that the individual was approximately 8 years old at death (~2939 days). Registry of developmental stress across the dentition allows the establishment of a developmental chronology (Figure 10), including ages at crown initiation and completion (see Table S2 in Smith et al., 2007[b]). Root extension rates for various teeth are given in Table 2. Anterior tooth root formation rates were found to be considerably higher than posterior rates.

4. Discussion

Crown formation times in the Scladina Juvenile permanent maxillary right first molar cusps are less than modern human first molar mean formation times (Smith et al., 2007[b, c], 2010), but are similar to chimpanzee times (Smith et al., 2007[d]). In the case of Neandertal molars,

	Row	Tooth	Cusp	Thick (um)	Min (days)	Max (days)	Pkg	Imb (days)	Total (days)
Scla 4A-11	**Maxillary**	I1	—	worn	n/a	n/a	~121	968	n/a
Scla 4A-14		I2	—	~800	211	281	~120	960	1206
Scla 4A-16		C	—	~825	217	288	~131	1048	1301
Scla 4A-2/P4 (unerupted)		P4	ling	995	242	327	n/a	n/a	n/a
			buc	775	189	265	n/a	n/a	n/a
Scla 4A-4		M1	mp	worn	n/a	n/a	n/a	n/a	872
			mb	worn	n/a	n/a	n/a	n/a	811*
Scla 4A-3		M2	mp	1260	307	396	77	616	967
			mb	1155	281	369	78	624	949
			dp	1220	297	386	74	592	933
			db	1300	316	405	71	568	929
Scla 4A-8		M3	mp	1265	308	397	54+	432	784+
			mb	1405	342	430	58+	464	850+
			mp	1260	307	396	48+	384	735+
			db	1315	320	409	45+	360	724+
Scla 4A-15	**Mandibular**	I1	—	worn	n/a	n/a	~95	760	n/a
Scla 4A-20		I2	—	worn	n/a	n/a	~101	808	n/a
Scla 4A-12		C	—	~660	174	239	~140	1120	1326
Scla 4A-6		P3	—	830	202	281	94	752	994
Scla 4A-1/P4 (unerupted)		P4	ling	890	217	298	n/a	n/a	n/a
			buc	915	223	305	n/a	n/a	n/a
Scla 4A-1/M1		M1	ml	worn	n/a	n/a	n/a	n/a	n/a
			mb	worn	n/a	n/a	n/a	n/a	n/a
Scla 4A-1/M2		M2	ml	965	235	319	n/a	n/a	n/a
			mb	1060	258	345	n/a	n/a	n/a
			dl	885	215	297	n/a	n/a	n/a
			db	1535	373	459	n/a	n/a	n/a
Scla 4A-1/M3 (unerupted)		M3	ml	905	220	303	n/a	n/a	n/a
			mb	905	220	303	n/a	n/a	n/a
			dl	1100	268	355	n/a	n/a	n/a
			db	1655	403	484	n/a	n/a	n/a

Table 1: Developmental variables for the Scladina juvenile tooth crowns. **Tooth** = central incisor (I1), lateral incisor (I2), canine (C), first premolar (P3), second premolar (P4), and first, second and third molars (M1, M2, & M3). For maxillary molar cusps (**Cusp**): 'mb' = mesiobuccal cusp (paracone), 'mp' = mesiopalatal cusp (protocone), 'db' = distobuccal cusp (metacone), 'dp' = distopalatal cusp (hypocone). For mandibular molar cusps: 'mb' = mesiobuccal cusp (protoconid), 'ml' = mesiolingual cusp (metaconid), 'db' = distobuccal cusp (hypoconid), 'dl' = distolingual cusp (entoconid). **Thick** = linear enamel thickness (in microns) taken from micro-CT slices. Slight estimations were made for light wear, as indicated by '~'. **Min** = cusp time derived from cuspal enamel thickness divided by 3.80 and 4.11 microns/day for anterior and posterior teeth respectively. **Max** = cuspal time derived from the use of regression equations (Dean et al., 2001; Schwartz & Dean, 2001). **Pkg** = perikymata, the number of long-period lines on the enamel surface counted from casts of the original teeth. Slight estimations were made for light wear, as indicated by '~'. **Imb** = total number of perikymata multiplied by 8. **Total** = crown formation time; mean cuspal enamel formation time plus the imbricational formation time. '*' Assumes an equal amount of prenatal formation as the permanent maxillary first molar mp cusp. 'worn' indicates that data are not available due to heavy attrition.

relatively short formation times may be explained in part by differences in cuspal enamel, which is approximately 60–90% thinner than in modern humans (Smith et al., 2007[b], 2010). Molar cuspal enamel formation times are likely to be shorter than in modern humans, as overall daily secretion rates do not vary between Neandertals and modern humans (Dean et al., 2001; Macchiarelli et al., 2006; Smith et al., 2009). Furthermore, coronal extension rates for first molar cusps were outside the range of modern human values, and were more similar to chimpanzee values (Smith et al., 2007[b], 2010). A similar pattern of thinner cuspal enamel and faster coronal extension was also found in a Neandertal third molar from Greece (Smith et al., 2009).

When the rest of the dentition is examined, it appears that certain Neandertal anterior teeth form over a greater period of time than modern human populations (e.g., permanent maxillary lateral incisor), however this is not the case for other anterior teeth (e.g., permanent mandibular canine) or the first premolar, which appear to form over shorter periods of time than modern human populations (Smith et al., 2007[b], 2010; Reid et al., 2008). Although similarities in perikymata

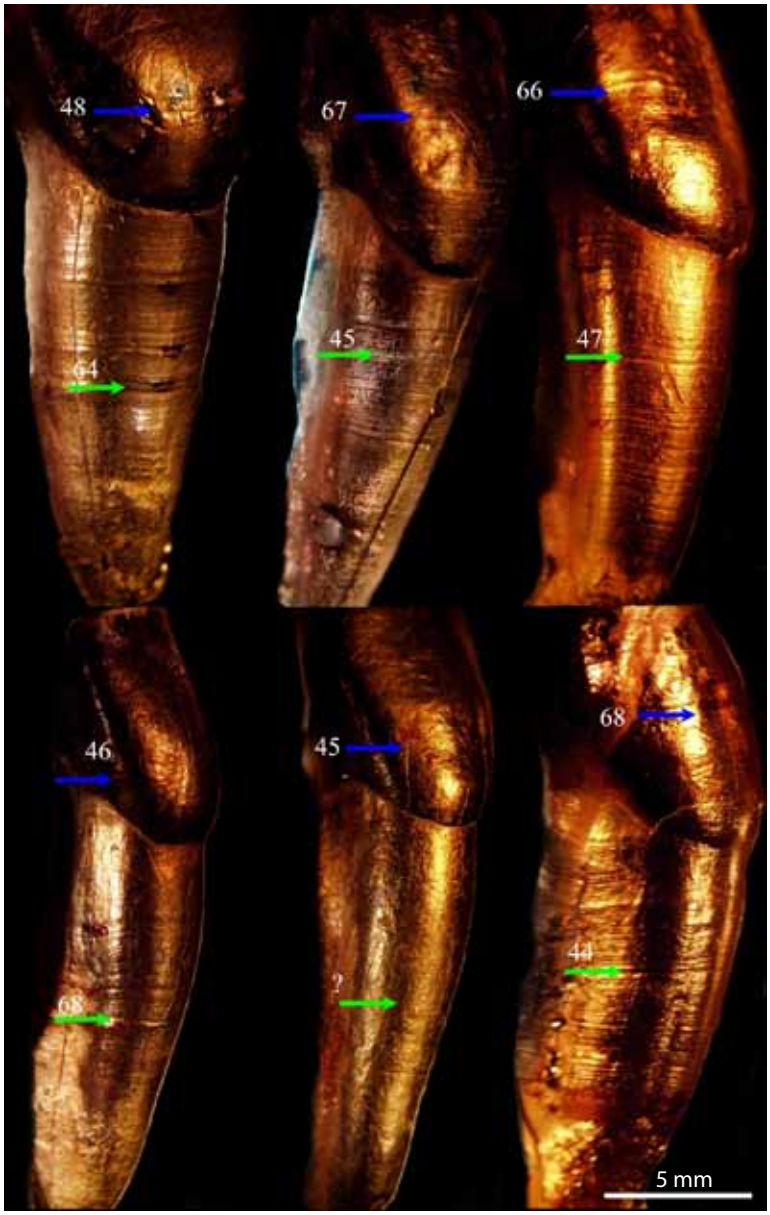

Figure 9: Developmental stress matched across the anterior dentition. From left to right (maxillary above, mandibular below) central incisor, lateral incisor, canine. The first stress event (blue arrow) was identified in the histological section of the permanent maxillary first molar at 875 days of age, with the number of subsequent perikymata after this event indicated on each tooth. The number of periradicular bands between the cervix and subsequent stress event (green arrow) is indicated, with 113 lines between events (904 days). Thus this second event occurred at 1779 days of age. Modified from Smith et al. (2007[b]).

numbers between Neandertals and modern humans have been noted (Guatelli-Steinberg & Reid, 2008), this study suggests that certain Neandertal teeth are characterized by shorter periods of overall crown formation, due to thinner cuspal enamel and greater rates of crown extension. Smith et al. (2007[b], 2010) suggested that

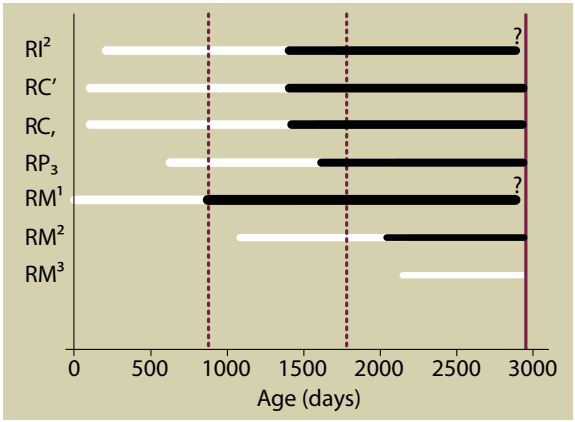

Figure 10: Developmental chronology of the Scladina Juvenile. Horizontal lines indicate crown formation (white) and root formation (black). The position of two stress events used to register teeth (see Figure 9) is indicated (dotted vertical lines), as well as death (solid vertical line). Given that the permanent maxillary lateral incisor and first molar had completed root formation prior to death, it was not possible to determine the end of root formation (indicated by '?'). Modified from Smith et al. (2007[b]).

anterior tooth formation times in Neandertals may also relate to their absolutely larger crowns.

Due to the lack of comparative hominoid root formation data, it is difficult to interpret root extension rates in the Scladina individual. This is further complicated by the fact that root extension rates vary within teeth and among tooth positions. Limited data on modern humans suggests that the first few millimetres of root formation takes place at ~3–4 microns/day (Dean & Beynon, 1991; Smith et al., 2007[a]), although the first few millimetres of human first molars may form at ~4–7 microns/day on average (Macchiarelli et

Tooth	Length	Rate
RI^1	5.94	11.6
RI^2	2.63	7.3
RC' (partial)	3.63	9.6
RC' (complete)	17.66	11.5
RM^1	13.59	*6.5
RM^2	5.83	6.4
RI_1	5.88	10.8
RI_2	6.03	11.1
RC, (partial)	4.04	11.5
RC, (complete)	16.38	10.8
RP_3	10.41	7.8

Table 2: Cumulative mean root extension rates for the Scladina individual's dentition. **Tooth** = right (R), central incisor (I1), lateral incisor (I2), canine (C), first premolar (P3), and first and second molars (M1 — palatal root, M2 — mesiobuccal root). **Length** is in mm, and **Rate** is in microns/day. Rates are for the length of root specified, measured from the enamel cervix apically. '*' Minimum rate: based on assumption that UM1 root completed formation at death.

Tooth	Scladina	Mean Pkg	Min	Max	N
RI^1	~121	138	121	161	10
RI^2	~120	143	133	156	9
RC′	~131	138	114	157	14
RM^2		96	77	117	11
RI_1	~95	134	118	158	5
$R1_2$	~101	147	110	177	8
RC,	~140	159	135	198	10
RP_3		109	88	130	5

Table 3: Comparison of perikymata number in the Scladina dentition with other Neandertals. **Tooth** = right dentition (R), central incisor (I1), lateral incisor (I2), canine (C), first premolar (P3) buccal cusp, and second molar (M2) mesiobuccal cusp. Slight estimations were made for light wear, as indicated by '~'. Mean pkg (**Mean Pkg**), minimum (**Min**), maximum (**Max**), and sample sizes are derived from Neandertal data in Guatelli-Steinberg & Reid (2008).

al., 2006; Dean, 2007[b]). Chimpanzee first molar roots may show similar or slightly faster rates of extension (Smith et al., 2007[d]). The minimum average root extension rate estimated for the Scladina permanent maxillary first molar palatal root (6.5 microns/day) is greater than similar data on modern human permanent mandibular first molars (6.1 microns/day: Dean, 2007[b]) or the La Chaise permanent mandibular molar (6.3 microns/day: Macchiarelli et al., 2006). Moreover, because the root had completed formation prior to death, it is quite likely that the average extension rate in the Scladina permanent maxillary first molar was greater than 6.5 microns/day. This may have led to an earlier age of M1 eruption, although it was not possible to determine this conclusively.

Perikymata numbers in the Scladina Juvenile fall either near the low end of values reported for other Neandertals, or below this range in the case of the permanent maxillary and mandibular lateral incisors and the permanent mandibular central incisor (Table 3). Comparisons of canine size between the Scladina Juvenile and the Obi-Rakhmat individual may indicate that sex differences influence Neandertal variation (Figure 11). Modern human females tend to show slightly younger ages of tooth initiation, eruption and completion (e.g., Smith, 1991; Liversidge, 2003), in addition to shorter canine crown formation times than males (Schwartz & Dean, 2001). Although it is tempting to suggest that the Scladina individual is a female (Toussaint, Chapter 9), potentially leading to some degree of advanced dental development, confirmation of this awaits recovery of associated postcranial material.

When the tooth calcification stages and eruption status of the Scladina Juvenile are compared modern human (Smith, 1991; Liversidge, 2003; Smith et al., 2010), it is clear that this individual is several years younger than a modern human juvenile at the same developmental stage. For example, the second molar is beyond clinical (gingival) occlusion; second molar eruption occurs on average at 10–13 years of age in global human populations. Advanced molar formation has previously been noted in Neandertals (Wolpoff, 1979; Tompkins, 1996). While early third molar initiation ages have been reported for modern humans of southern African origin (Liversidge, 2008), we conclude that age at death in Neandertals should not be assessed by comparison with modern human standards, particularly those derived from European or North American populations. The recovery of postcranial material from the Scladina Juvenile would be a welcome complement to this study, particularly given debates over differences in relative skeletal versus dental ages of other well-preserved hominins (e.g. Devil's Tower, Le Moustier 1, Narikotome).

Acknowledgements

We are grateful to Nora De Clerck, Heiko Temming, Andreas Winzer, and the ID 19 beamline staff for technical support. This research was supported by the Max Planck Society, EU FP6 Marie Curie Actions MRTN-CT-2005-019564, the University of Liège, the city of Andenne, the Direction de l'Archéologie of the Service public de Wallonie in Belgium, the European Synchrotron Radiation Facility, and Harvard University.

Figure 11: Permanent maxillary canine size variation in Neandertals from Scladina (Scla 4A-18; left) and Obi Rakhmat Grotto (right, cast of original).

References

Boyde A., 1963. Estimation of age at death of young human skeletal remains from incremental lines in the dental enamel. *Third International Meeting in Forensic Immunology, Medicine, Pathology, and Toxicology*, London, April 1963: 16–24.

Boyde A., 1989. Enamel. In A. Oksche & L. Vollrath (eds.), *Handbook of Microscopic Anatomy*, V, 6: Teeth. Berlin, Springer-Verlag: 309–473.

Boyde A., 1990. Developmental interpretations of dental microstructure. In C. J. DeRousseau (ed.), *Primate Life History and Evolution*. New York, Wiley-Liss: 229–267.

Bromage T. G., 1991. Enamel incremental periodicity in the pig-tailed macaque: a polychrome fluorescent labeling study of dental hard tissues. *American Journal of Physical Anthropology*, 86: 205–214.

Bromage T. G. & Dean M. C., 1985. Re-evaluation of the age at death of immature fossil hominids. *Nature*, 317: 525–527.

Coqueugniot H. & Hublin J.-J., 2007. Endocranial volume and brain growth in immature Neandertals. *Periodicum Biologorum*, 109: 379–385.

Dean M. C., 1995. The nature and periodicity of incremental lines in primate dentine and their relationship to periradicular bands in OH 16 (*Homo habilis*). In J. Moggi Cecchi (ed.), *Aspects of Dental Biology: Paleontology, Anthropology and Evolution*. Florence, International Institute for the Study of Man: 239–265.

Dean M. C., 2007[a]. Dental development and life history in primates and a comparison of cuspal enamel growth trajectories in a specimen of *Homo erectus* from Java (Sangiran S7-37), a Neandertal (Tabun C1), and an early *Homo sapiens* specimen (Skhul II), from Israel. In M. Faerman, L. K. Horwitz, T. Kahana & U. Zilberman (eds.), *Faces from the past: diachronic patterns in the biology of human populations from the eastern Mediterranean*. Oxford, British Archaeological Reports, International Series, 1603: 21–27.

Dean M. C., 2007[b]. A radiographic and histological study of modern human lower first permanent molar root growth during the supraosseous eruptive phase. *Journal of Human Evolution*, 53: 635–646.

Dean M. C. & Beynon A. D., 1991. Histological reconstruction of crown formation times and initial root formation times in a modern human child. *American Journal of Physical Anthropology*, 86: 215–228.

Dean M. C., Beynon A. D., Thackeray J. F. & Macho G. A., 1993. Histological reconstruction of dental development and age at death of a juvenile Paranthropus robustus specimen, SK 63, from Swartkrans, South Africa. *American Journal of Physical Anthropology*, 91: 401–419.

Dean M. C., Leakey M. G., Reid D. J., Schrenk F., Schwartz G. T., Stringer C. B. & Walker A., 2001. Growth processes in teeth distinguish modern humans from *Homo erectus* and earlier hominins. *Nature*, 414: 628–631.

Dean M. C., Stringer C. B. & Bromage T. G., 1986. Age at death of the Neanderthal child from Devil's Tower, Gibraltar and the implications for studies of general growth and development in Neanderthals. *American Journal of Physical Anthropology*, 70: 301–309.

Fitzgerald C. M., 1998. Do enamel microstructures have regular time dependency? Conclusions from the literature and a large-scale study. *Journal of Human Evolution*, 35: 371–386.

Granat J. & Heim J.-L., 2003. Nouvelle méthode d'estimation de l'âge dentaire des Néandertaliens. *L'Anthropologie*, 107: 171–202.

Guatelli-Steinberg D. & Reid D. J., 2008. What molars contribute to an emerging understanding of lateral enamel formation in Neandertals vs. modern humans. *Journal of Human Evolution*, 54: 236–250.

Guatelli-Steinberg D., Reid D. J., Bishop T. A. & Larsen C. S., 2005. Anterior tooth growth periods in Neanderthals were comparable to those of modern humans. *Proceedings of the National Academy Science of the United States of America*, 102, 40: 14197–14202.

Guatelli-Steinberg D., Reid D. J. & Bishop T. A., 2007[a]. Did the lateral enamel of Neandertal anterior teeth grow differently from that of modern humans? *Journal of Human Evolution*, 52: 72–84.

Guatelli-Steinberg D., Reid D. J., Bishop T. A. & Larsen C. S., 2007[b]. Imbricational enamel formation in Neandertals and recent modern humans. In S. E. Bailey & J.-J. Hublin (eds.), *Dental Perspectives on Human Evolution: State of the Art Research in Dental Paleoanthropology*.

Dordrecht, Springer: 211–227.

Liversidge H. M., 2003. Variation in modern human dental development. In J. L. Thompson, G. E. Krovitz & A. J. Nelson (eds.), *Patterns of Growth and Development in the Genus Homo*, Cambridge University Press: 73–113.

Liversidge H. M., 2008. Timing of human mandibular third molar formation. *Annals of Human Biology*, 35: 294–321.

Macchiarelli R., Bondioli L., Debénath A., Mazurier A., Tournepiche J.-F., Birch W. & Dean C., 2006. How Neandertal molar teeth grew. *Nature*, 444: 748–751.

Mann A. E., Monge J. M. & Lampl M., 1991. Investigation into the relationship between perikymata counts and crown formation times. *American Journal of Physical Anthropology*, 86: 175–188.

Mann A. & Vandermeersch B., 1997. An adolescent female Neandertal mandible from Montgaudier Cave, Charente, France. *American Journal of Physical Anthropology*, 103: 507–527.

Olejniczak A. J., Smith T. M., Feeney R. N. M., Macchiarelli R., Mazurier A., Bondioli L., Rosas A., Fortea J., de la Rasilla M., García-Tabernero A., Radovčić J., Skinner M. M., Toussaint M. & Hublin J.-J., 2008. Dental tissue proportions and enamel thickness in Neandertal and modern human molars. *Journal of Human Evolution*, 55: 12–23.

Ramirez Rozzi F. V., 1993. Microstructure and development of the enamel tooth of the Neanderthal from Zafarraya, Spain. *Comptes Rendus de l'Académie des Sciences de Paris*, 316: 1635–1642.

Ramirez Rozzi F. V., 2005. Age at death of the Neanderthal child from Hortus. *Bulletins et Mémoires de la Société d'Anthropologie de Paris*, 17: 47–55.

Ramirez Rozzi F. V. & Bermudez de Castro J. M., 2004. Surprisingly rapid growth in Neanderthals. *Nature*, 428: 936–939.

Reid D. J. & Dean M. C., 2006. Variation in modern human enamel formation times. *Journal of Human Evolution*, 50: 329–346.

Reid D. J., Guatelli-Steinberg D. & Walton P., 2008. Variation in modern human premolar enamel formation times: Implications for Neandertals. *Journal of Human Evolution*, 54: 225–235.

Reid D. J., Schwartz G. T., Dean C. & Chandrasekera M. S., 1998. A histological reconstruction of dental development in the common chimpanzee, Pan troglodytes. *Journal of Human Evolution*, 35: 427–448.

Sasaki C., Suzuki K., Mishima H. & Kozawa Y., 2003. Age determination of the Dederiyeh 1 Neanderthal child using enamel cross-striations. In T. Akazawa & S. Muhesen (eds.), *Neanderthal Burials: Excavations of the Dederiyeh Cave, Afrin, Syria*. Kyoto, International Research Center for Japanese Studies: 263–267.

Schwartz G. T. & Dean C., 2001. Ontogeny of canine dimorphism in extant hominoids. *American Journal of Physical Anthropology*, 115: 269-283.

Schwartz G. T., Reid D. J. & Dean C., 2001. Developmental aspects of sexual dimorphism in hominoid canines. *International Journal of Primatology*, 22: 837–860.

Shackelford L. L., Stinespring Harris A. E. & Konigsberg L. W., 2012. Estimating the distribution of probable age-at-death from dental remains of immature human fossils. *American Journal of Physical Anthropology*, 147: 227–253.

Smith B. H., 1991. Standards of human tooth formation and dental age assessment. In M. S. Kelley & C. S. Larsen (eds.), *Advances in Dental Anthropology*. New-York, Wiley-Liss: 143–168.

Smith T. M., 2006. Experimental determination of the periodicity of incremental features in enamel. *Journal of Anatomy*, 208: 99–114.

Smith T. M., 2008. Incremental dental development: methods and applications in hominoid evolutionary studies. *Journal of Human Evolution*, 54: 205-224.

Smith T. M., Harvati K., Olejniczak A. J., Reid D. J., Hublin J.-J. & Panagopoulou E., 2009. Brief communication: Dental development and enamel thickness in the Lakonis Neanderthal molar. *American Journal of Physical Anthropology*, 138: 112–118.

Smith T. M., Olejniczak A. J., Tafforeau P. T., Reid D. J., Grine F. E. & Hublin J.-J., 2006[b]. Molar crown thickness, volume, and development in South African Middle Stone Age humans. *South African Journal of Science*, 102: 513–517.

Smith T. M., Olejniczak A. J., Zermeno J. P., Tafforeau P. T., Skinner M. M., Hoffmann A., Radovčić J., Toussaint M., Kruszynski R., Menter C., Moggi-Cecchi J., Glasmacher U. A.,

Kullmer O., Schrenk F., Stringer C. B. & Hublin J.-J., 2012. Variation in enamel thickness within the genus Homo. *Journal of Human Evolution*, 62: 395–411.

Smith T. M., Reid D. J., Dean M. C., Olejniczak A. J., Ferrell R. J. & Martin L. B., 2007[b]. New perspectives on chimpanzee and human dental development. In S. E. Bailey & J.-J. Hublin (eds.), *Dental Perspectives on Human Evolution: State of the Art Research in Dental Paleoanthropology*. Dordrecht, Springer: 177–192.

Smith T. M., Reid D. J., Dean M. C., Olejniczak A. J. & Martin L. B., 2007[d]. Molar development in common chimpanzees (*Pan troglodytes*). *Journal of Human Evolution*, 52: 201–216.

Smith T. M., Reid D. J., Olejniczak A. J., Bailey S., Glantz M., Viola B. & Hublin J.-J., 2011. Dental development and age at death of a Middle Paleolithic juvenile hominin from Obi-Rakhmat Grotto, Uzbekistan. In S. Condemi & G. C. Weniger, (eds.), *Continuity and Discontinuity of the Peopling of Europe. One Hundred Fifty Years of Neanderthal Study*. Dordrecht, Springer: 155–164.

Smith T. M., Reid D. J. & Sirianni J. E., 2006[a]. The accuracy of histological assessments of dental development and age at death. *Journal of Anatomy*, 208: 125–138.

Smith T. M. & Tafforeau P. T., 2008. New visions of dental tissue research: tooth development, chemistry, and structure. *Evolutionary Anthropology*, 17: 213–226.

Smith T. M., Tafforeau P. T., Reid D. J., Grün R., Eggins S., Boutakiout M. & Hublin J.-J., 2007[a]. Earliest evidence of modern human life history in North African early *Homo sapiens*. *Proceedings of the National Academy Science of the United States of America*, 104, 15: 6128–6133.

Smith T. M., Tafforeau P. T., Reid D. J., Pouech J., Lazzari V., Zermeno J. P., Guatelli-Steinberg D., Olejniczak A. J., Hoffman A., Radovčić J., Masrour M., Toussaint M., Stringer C. B. & Hublin J.-J., 2010. Dental evidence for ontogenetic differences between modern humans and Neanderthals. *Proceedings of the National Academy of Sciences of the United States of America*, 107, 49: 20923–20928.

Smith T. M., Toussaint M., Reid D. J., Olejniczak A. J. & Hublin J.-J., 2007[c]. Rapid dental development in a Middle Paleolithic Belgian Neanderthal. *Proceedings of the National Academy Science of the United States of America*, 104, 51: 20220–20225.

Stringer C. B. & Dean M. C., 1997. Age at death of Gibraltar 2 — a reply. *Journal of Human Evolution*, 32: 471–472.

Stringer C. B., Dean M. C. & Martin R. D., 1990. A comparative study of cranial and dental development within a recent British sample and among Neandertals. In C. J. DeRousseau (ed.), *Primate Life History and Evolution*. Wiley-Liss, New York: 115–152.

Tafforeau P. T., 2004. *Phylogenetic and functional aspects of tooth enamel microstructure and three-dimensional structure of modern and fossil primate molars: contributions of X-ray synchrotron microtomography*. PhD Thesis, Université de Montpellier II.

Tafforeau P. T., Bentaleb I., Jaeger J.-J. & Martin C., 2007. Nature of laminations and mineralization in rhinoceros enamel using histology and X-ray synchrotron microtomography: potential implications for palaeoenvironmental isotopic studies. *Palaeogeography, Palaeoclimatology, Palaeoecology*, 246: 206–227.

Tafforeau P. T., Boistel R., Boller E., Bravin A., Brunet M., Chaimanee Y., Cloetens P., Feist M., Hoszowska J., Jaeger J.-J., Kay R. F., Lazzari V., Marivaux L., Nel A., Nemoz C., Thibault X., Vignaud P. & Zabler S., 2006. Applications of X-ray synchrotron microtomography for non-destructive 3D studies of paleontological specimens. *Applied Physics* A, 83, 2: 195–202.

Tafforeau P. T. & Smith T. M., 2008. Nondestructive imaging of hominoid dental microstructure using phase contrast X-ray synchrotron microtomography. *Journal of Human Evolution*, 54: 272–278.

Thompson J. L. & Nelson A. J., 2000. The place of Neandertals in the evolution of hominid patterns of growth and development. *Journal of Human Evolution*, 38: 475–495.

Tillier A.-M., 2000. Palaeoauxology applied to Neanderthals. Brno, *Anthropologie*, 38: 109–120.

Tompkins R. L. 1996. Relative dental development of Upper Pleistocene hominids compared to human population variation. *American Journal of Physical Anthropology*, 99: 103–118.

Wolpoff M. H., 1979. The Krapina dental remains. *American Journal of Physical Anthropology*, 50: 67–114.